Field dependence of spin excitations in NiFe/Cu/NiFe trilayered circular dots

G. Gubbiotti*
Research Center SOFT-INFM-CNR, Universita' di Roma "La Sapienza," I-00185 Roma, Italy

M. Madami and S. Tacchi
Dipartimento di Fisica, Università di Perugia, Via A. Pascoli, 06123 Perugia, Italy
and INFM, Via A. Pascoli, 06123 Perugia, Italy

G. Carlotti
INFM-CNR Research Center S3, Via Campi 213/a, 41100, Modena, Italy
and Dipartimento di Fisica, Universita' di Perugia, Via A. Pascoli, 06123 Perugia, Italy

T. Okuno
Institute for Chemical Research, Kyoto University, Uji 611-0011, Japan
(Received 12 January 2006; revised manuscript received 1 March 2006; published 28 April 2006)

Brillouin light scattering has been exploited to study the magnetic normal modes of trilayered circular dots (radius 100 nm), consisting of a pair of 10 nm thick permalloy layers separated by a Cu spacer with thickness of 10 nm. The field evolution of both the frequencies and the profiles of the spin-wave modes was investigated over a wide range of applied fields, encompassing both the parallel alignment of the layers magnetizations at saturation and the in-plane antiparallel state at remanence. The experimental data have been satisfactorily reproduced using a micromagnetic approach which solves the discretized Landau-Lifshitz-Gilbert equation over the layered structure in the time domain and then performs a local Fourier transform.

DOI: 10.1103/PhysRevB.73.144430 PACS number(s): 75.75.+a, 75.30.Ds, 78.35.+c

I. INTRODUCTION

The discovery of giant magnetoresistance combined with advanced micro- and nanofabrication technologies led to rapid advances in the development of magnetic data-storage devices.[1] The high speed operation of these devices in the gigahertz frequency range requires a detailed understanding and controlling of the dynamics of submicrometric magnetic elements because it has been shown that their switching time is determined by the eigenfrequencies of dynamic excitations (spin waves) inside the elements.[2] In the past years, several works appeared dealing with the magnetic eigenmodes of micrometer-sized ferromagnetic elements both in single-domain[3–5] and the vortex state.[5–12] Lateral spatial confinement and inhomogeneous internal magnetic field lead to quantized and localized modes, respectively.[13,14]

However, significantly less is known about the eigenmode spectrum of laterally confined elements having a layered structure, as for instance, in spin-valve elements, where two ferromagnetic layers are separated by a nonmagnetic spacer. The dynamics of such elements is expected to be different from that measured in single-layer magnetic film due to large magnetostatic fields, interlayer coupling, and different magnetic excitation spectra of the layers. The magnetostatic modes of tangentially magnetized NiFe/Cu/NiFe and Fe/Au/Fe stripes have been recently investigated by Brillouin light scattering (BLS) from thermally excited spin waves in the case of pure dipolar[15] and exchange coupling[16] between the ferromagnetic layers. More recently, an interesting theoretical paper about the dynamics of coupled vortices in layered magnetic nanodots has been published by Guslienko *et al.*,[17] studying the low-frequency motion of the two vortex cores. To the best of our knowledge, neither experimental nor theoretical papers have been published to date about the resonance frequencies of the spin excitations of layered magnetic dots.

To fill this lack of data, in this work we apply the BLS technique to investigate the excitation spectra of trilayered NiFe(10 nm)/Cu(10 nm)/NiFe(10 nm) disk-shaped dots. Several spin modes are observed in the measured spectra and their frequencies tracked as a function of the intensity of the applied magnetic field. Information about the equilibrium magnetization state corresponding to different values of applied fields has been gained by the magneto-optical Kerr effect (MOKE) measurements. In order to reproduce the measured data, we did micromagnetic simulations of both the magnetization curve and the eigenmode spectrum, using the three-dimensional version of the Object Oriented Micro-Magnetic Framework (OOMMF) developed at NIST.[18]

II. EXPERIMENTAL DETAILS

NiFe(10 nm)/Cu(10 nm)/NiFe(10 nm) trilayer has been deposited on a commercial oxidized Si wafer by thermal evaporation. Then, a 2×2 mm^2 squared array of disk-shaped dots was fabricated by a combination of e-beam lithography, e-beam evaporation, and lift-off processes.[19] Both the dot diameter and the interdot spacing is 200 nm, corresponding to a repetition period of 400 nm. Magnetic hysteresis loops were measured in the longitudinal Kerr effect configuration, i.e., with the external field applied in the sample plane and parallel to the [10] direction of the dots lattice. The nearly crossed polarizers method was used, including a laser modu-

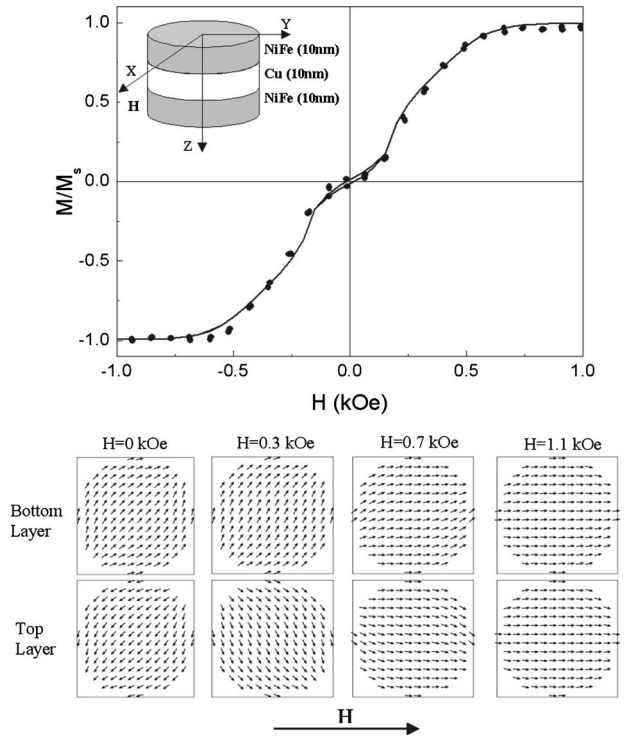

FIG. 1. Upper panel: measured longitudinal MOKE (full points) and simulated hysteresis loop (continuous curve) for the trilayered dots. The layering scheme of the sample, the direction of the applied field H and the orientation of the Cartesian coordinate system used for calculations are shown as well. Bottom panel: magnetization configurations in the two (top and bottom) NiFe disks for different values of the external magnetic field H whose direction is represented by the arrow.

lated in amplitude at 450 Hz and a lock-in amplifier.[20] Room temperature Brillouin light scattering spectra were recorded in the backscattering geometry using a Sandercock-type (3+3)-pass tandem interferometer[21] and the 532 nm line of a single-mode diode-pumped solid-state laser. A dc magnetic field, variable in the range 0–1.5 kOe, was applied in the sample plane along the X direction (see Fig. 1) and perpendicular to the scattering plane of light. The incidence angle of light was fixed to 10°. Cross polarizations between the incident and the scattered beams were adopted in order to minimize the phonon contribution to the spectra. Part of the NiFe/Cu/NiFe trilayer was left unpatterned and used as reference sample to determine the magnetic parameter of permalloy used in the micromagnetic simulations.

III. MICROMAGNETIC SIMULATIONS

In the numerical OOMMF micromagnetic package (version 1.2.0.4), the dots are discretized into a two-dimensional grid of 5×5 nm^2 cell size so that each layer is described by 1600 cells. The height of the cells is equal to the thickness of each layer (10 nm), i.e., we assume only negligible variations of the magnetization perpendicular to the element plane due to the small thickness of the layers. The equilibrium distribution of the magnetization for a given value of the applied field if found by numerically integrating the Landau-Lifshitz-Gilbert and stopping the integration when the torque $M\times H$ reaches a sufficiently low value so that the condition $|M\times H|/M_s^2\leqslant10^{-5}$ is fulfilled. The permalloy parameters used in the simulations are: $A=13\times10^{-12}$ J/m for the exchange stiffness and zero magnetocrystalline anisotropy. To find the equilibrium configuration of the magnetization, the damping parameter was set to $\alpha=0.5$. To break the symmetry due to fact the dots consist of two nominally identical permalloy layers, we used slightly different values of the saturation magnetization in the two ferromagnetic layers, namely $M_S=800\times10^3$ A/m and $M_S=790\times10^3$ A/m. This is physically sound since the top NiFe layer, being exposed to air, may have a reduced magnetization because of unavoidable oxidation. Since the Cu spacer is relatively thick, the case of purely dipolar interlayer coupling has been considered, excluding any exchange coupling between the permalloy layers. In addition, no interaction between different elements of the array has been considered, being the interdot spacing larger than the dots radius.[22] To calculate the resonance frequencies of the system the resulting spin configuration obtained by OOMMF for every value of the static magnetic field is used as the initial state for the dynamic calculation. Retaining the value of in-plane dc uniform field, which is constant in time and directed along the positive X axis, the system was excited by an out-of-plane (Z direction) Gaussian pulse with a full width at half maximum of 1 ps and an amplitude of 10 Oe. Gaussian field pulses with the same temporal profile and with different spatial symmetries were used to highlight different modes. In particular, in addition to the uniform field pulse, we used pulses with either even or odd symmetry with respect to the X and Y directions.

After the field pulse the system was left free to evolve following the Landau-Lifshitz equation of motion with a damping factor set to $\alpha=0.00001$ and an effective gyromagnetic ratio $\gamma=2.31\times10^5$ m/A s. Since in the OOMMF calculations are performed at $T=0$ K, where thermally activated spin waves are not excited, such a small value of the damping parameter is necessary to observe the magnetization oscillations over several periods.

The time evolution of the three dynamic magnetization components (m_β with $\beta=X$, Y, and Z) (Ref. 23) was tracked over the next 5 ns by saving the configuration of the magnetization in each cell at uniform time steps (Δt) of 5 ps. Then, a Fourier analysis of the magnetization ringdown in each single cell of each layer enabled us to calculate the local power spectra of the magnetization components which are defined as follows:[4]

$$S_\beta(\vec{r}_i,\omega)=\left|\sum_j m_\beta(\vec{r}_i,t_j)\exp(i2\pi\omega t_j)\right|^2,$$

where $\vec{r}_i$ defines the position of each cell of the system and t_j is the simulation time. The index $j=1,2,\ldots,1000$ labels the jth time step. After that, the average power spectrum has been calculated summing the local power spectra over i,

$$\bar{S}_\beta(\omega)=\sum_i S_\beta(\vec{r}_i,\omega).$$

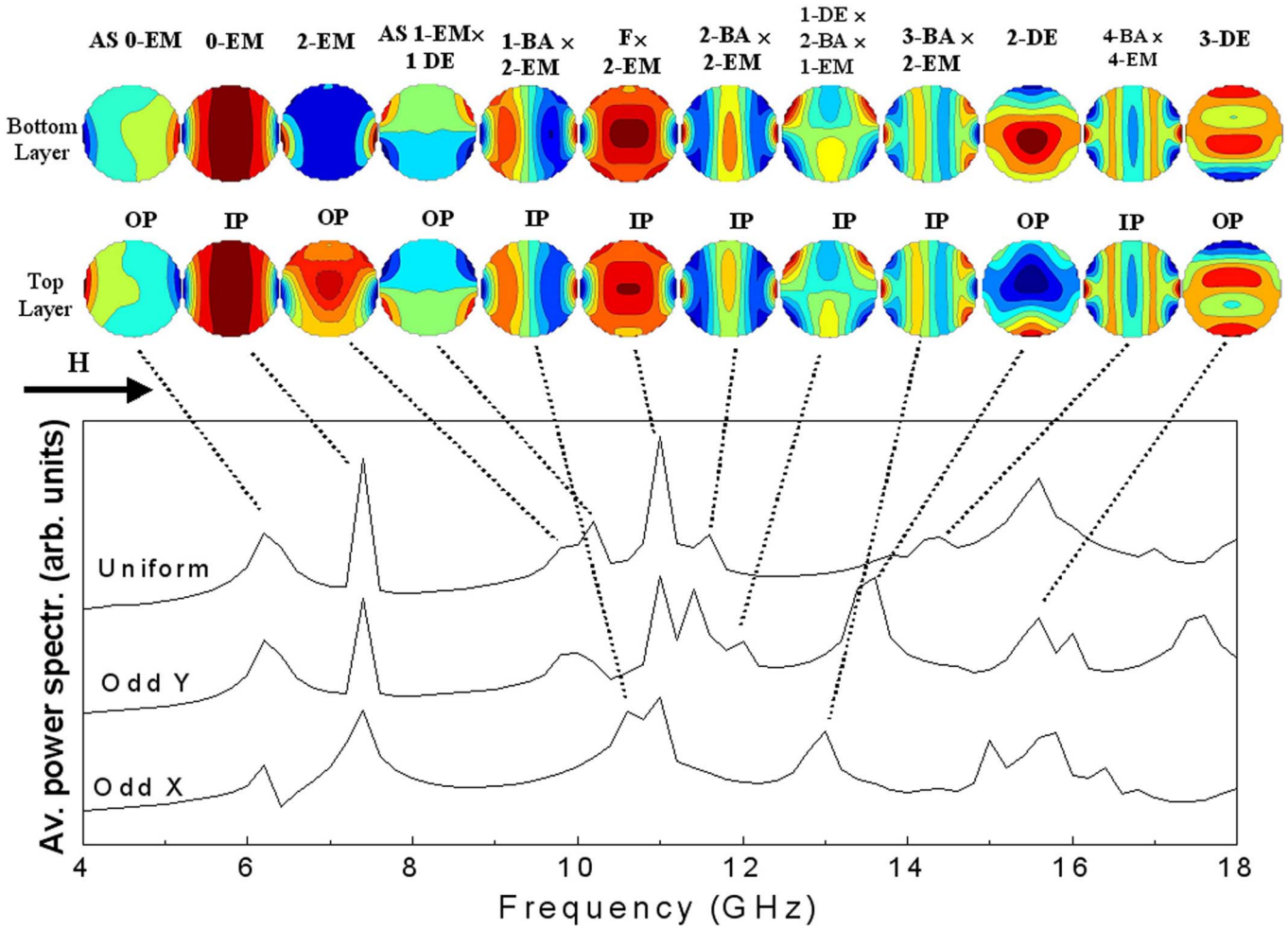

FIG. 2. (Color online) Calculated average power spectra obtained with an external static field $H=1.5$ kOe for different excitation pulses as described in the labels, i.e., for uniform pulse, and for X-odd symmetric and Y-odd symmetric pulses. The modes profiles in the two layers as well as the direction of the applied magnetic field H are shown in the upper part.

Several peaks are present in $\bar{S}_\beta(\omega)$ of both the top and bottom ferromagnetic disks, corresponding to eigenfrequencies for the oscillating component m_β; a surface plot of the real part of the Fourier coefficients for each eigenfrequency provides the profile of the corresponding eigenmode.

Similarly to the acoustic and optical modes assignment in a continuous (unpatterned) trilayer consisting of two ferromagnetic films separated by a nonmagnetic spacer, the calculated modes can be primarily classified according to whether the precessional motion of the dynamic magnetizations in the two ferromagnetic disks is in-phase (IP) or out-of-phase (OP).

Each of the above mentioned modes can be further classified according to the dynamical magnetization distribution within each layer (disk):[5,25] (i) modes localized near the particle ends in the direction of the applied magnetic field (end modes, n-EM); (ii) modes with nodal lines perpendicular to **H** (backwardlike modes, m-BA); (iii) modes with nodal lines parallel to the direction of **H** (Damon-Eshbach-type modes, n-DE); and (iv) modes with both parallel and perpendicular nodal lines (mixed modes). The integer numbers m (n) specify the number of nodal lines parallel (perpendicular) to the magnetization. The "mixed" modes (iv) are labeled m-BA$\times n$-DE. The mode with no nodal lines is the fundamental one (F), analogous to the Kittel uniform mode detected in a Ferromagnetic resonance (FMR) experiment.[24] Please note that this classification scheme is a useful but simplified approximation, because interlayer dipolar coupling can introduce a distortion of the mode profiles as well as specific features which prevent an unambiguous fit to the above classification.

Figure 2 reports the average power spectra for the NiFe/Cu/NiFe disk-shaped dots, calculated for an out-of-plane (Z direction) field pulse in the presence of a 1.5 kOe uniform dc magnetic field applied along the X direction. First of all, we have verified that applying excitation pulses with different symmetries in the XY plane allows the excitation of different normal modes.[4] For example, either the DE-like or the BA-like modes with an odd number of nodal lines, can be efficiently excited by using a perpendicular pulse with odd symmetry with respect to the Y and X axis, respectively. In the top panel of Fig. 2 the profiles of the excited normal modes for the bottom and top NiFe dots are shown. Here one can notice that the 2-DE mode is excited by the Y-odd pulse while the 3-BA$\times$2-EM is excited by the X-odd pulse, only.

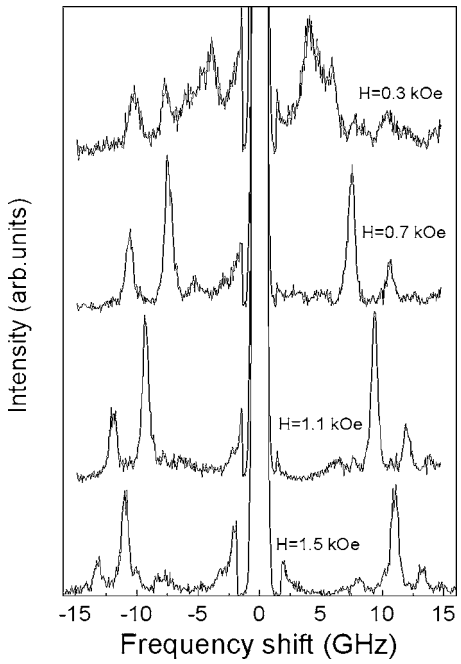

FIG. 3. Room temperature BLS spectra for different values of the external applied field.

These modes are not present at all or are very small in the power spectrum obtained for the system excited by the uniform pulse. Both the fundamental and the localized modes are excited by pulses with any symmetry. These latter are edge modes (0-EM) with the difference that the former is asymmetric (AS) inside each layer (with zero net dynamic magnetization) while the latter is symmetric (non zero net dynamic magnetization).

The large number of modes present in the frequency range investigated by BLS makes it impossible to perform a mode assignment just based on their frequency. The interpretation of the BLS spectra requires, therefore, the calculation of the normal mode profiles and of the BLS cross section.[25] To this aim, we have chosen to evaluate the Z component of the dynamical magnetization, i.e., the one perpendicular to the sample plane, because it gives the main contribution to the BLS cross section. [The Y component of the dynamical magnetization gives a negligible contribution, otherwise a marked Stokes/anti-Stokes asymmetry should be seen in the measured spectra of Fig. 3 (Ref. 25).] Assuming that the main contribution to the cross section is given by the top layer, which is quite reasonable because of the large attenuation of light reaching the bottom layer, and reminding the qualitative discussion presented in Ref. 25, we found that only a few modes, namely, the 0-EM, 2-EM, F$\times$2-EM, 2-DE, and 3-DE, are active in the scattering process and give a substantial contribution in the BLS spectra. For this reason, in the comparison with the experimental frequencies, we have followed the field dependence of the above mentioned five modes, only.

IV. RESULTS AND DISCUSSION

The first step of our magnetic characterization was to measure the longitudinal hysteresis loop for the array of layered dots, as described in Sec. II. Figure 1 shows the comparison between the experimental (points) and the calculated (continuous curve) loops. The hysteresis curve is characterized by an almost anhysteretic behavior which can be well reproduced by our calculation. The simulated magnetic configurations inside the dots as a function of the applied field are also shown in Fig. 1, bottom panels. The sample is initially saturated in a positive field $H=1.5$ kOe, corresponding to a parallel alignment of the layers magnetizations. These remain aligned as the field intensity is decreased down to 0.6 kOe, but when the field is further reduced, the layers magnetizations start to rotate in opposite directions until they reach a perfect anti-parallel alignment at zero field, with the layers magnetization at almost 45° with respect to the direction of the external applied field. This antiparallel domain configuration at remanence is clearly due to the dipolar interaction between the layers, which forces them to be antiparallel in the absence of field. Note however, that the choice of just 45° orientation as the final configuration at $H=0$, can be induced by the square shape of the discretized cells, which artificially introduces a slight biaxial in-plane anisotropy. It is important to notice that, during the reversal, the magnetization in each layer remains almost in single-domain state. This is different from the recent findings of other works on thicker trilayers,[17,26] where evidence of vortex formation in the disks was found.

To study the magnetic normal modes properties, we measured the BLS spectra with the applied magnetic field in the range 0–1.5 kOe. On both the Stokes and the anti-Stokes sides of the spectrum several well resolved peaks are seen (Fig. 3), whose relative intensity changes as a function of the external applied field. These modes are dispersionless, i.e., their frequency does not change as a function of the incidence angle of light, as typical for resonant modes in a laterally confined magnetic system. Moreover, no angular dependence of the spin mode frequency on the in-plane direction of the applied magnetic field has been observed for saturated dots. This enables us to exclude any appreciable in-plane anisotropy of the dots, as expected for isolated, circular dots of permalloy. For an applied field of 1.5 kOe, which ensures saturation of the dots, the five detected modes are identified as:

(1) The IP-0-EM (at 8 GHz) and the OP-2-EM (at 10 GHz), both of which have an amplitude concentrated close to the dot edge; (note, however, that the latter mode presents also a slight oscillation in the central part of the layer which makes it very similar to the 2-BA mode observed in Ref. 5 for a single layer circular dot).

(2) The very intense fundamental mode mixed with an end mode IP-F$\times$2-EM (at 11 GHz), which is almost uniform and with no nodes.

(3) The OP-2-DE mode (at 13.4 GHz) and OP-3-DE mode (at 15.8 GHz), characterized by the presence of nodal lines perpendicular to the direction of the magnetic field.

As stated in Sec. II, this assignment of the mode character to the measured modes has been done following two criteria:

(1) the proximity of the calculated frequency to the measured one, and

(2) the estimate of the BLS cross section, essentially linked to the square of the average dynamical magnetization

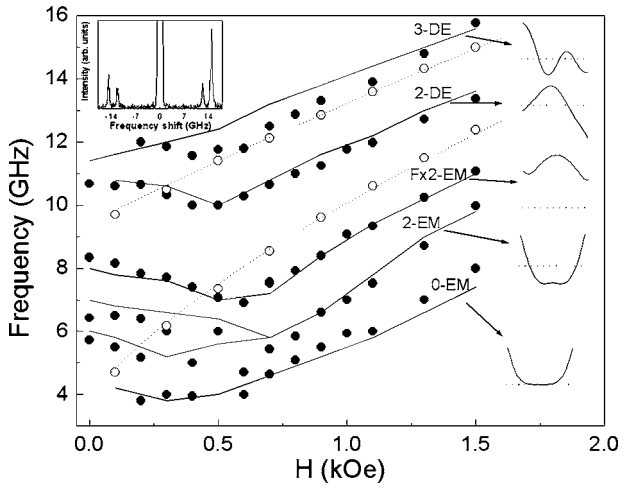

FIG. 4. Field dependence of the measured (full points) and calculated (continuous curves) spin modes frequency measured by the BLS for the NiFe/Cu/NiFe disk-shaped dots. The labels indicate the character of the modes whose contour plots are reported in Fig. 2 and the inset on the right shows a middle section of the dynamic magnetization m_z for the top layer along the oscillation direction: X direction for the 0-EM, 2-EM and fundamental mode and Y direction for the 2-DE and 3-DE modes. The horizontal dotted line signs the zero of the dynamic magnetization. The measured (open points) and fitted (dotted curves) frequencies for the unpatterned trilayer are also reported, as a reference. The inset shows a typical BLS spectrum for the unpatterned NiFe/Cu/NiFe trilayer for an applied field of 1.5 kOe. The two peaks correspond to the acoustic and optic spin modes.

of the top layer (this is not the same as the power spectrum of Fig. 2, since it contains the average of the square modulus of the magnetization, so it overestimates the cross sections of dots characterized by the presence of nodes).

For example, the mode at about 15.8 GHz has been classified as a 3-DE mode. This might seem to be strange since in previous investigations of single-layer circular dots,[5] we found the 2-DE mode to a visible in the spectra, instead of the 3-DE mode; this was characterized by a vanishing cross section, as expected for a mode with an odd number of nodes. The reason for this apparent discrepancy is that in the present case the mode profile inside one layer is appreciably modified by the dipolar coupling with the other magnetic layer, so that the average magnetization is far from vanishing for this distorted profile. To stress these considerations, a plot of the dynamic magnetization m_z across a middle section of the top layer is shown as inset in Fig. 4, where the comparison between the measured and the calculated frequencies is also reported. For the sake of comparison, we have also plotted as open symbols the frequency evolution of the acoustic and optical modes measured in the unpattened NiFe/Cu/NiFe trilayer. As seen in Fig. 4, on reducing the field intensity, the frequency of all the modes monotonously decreases and reaches a minimum at about 0.6 kOe, which corresponds to the saturation field (see Fig. 1). On further decreasing the field intensity, the frequencies of the modes start to increase again, reflecting the simultaneous and opposite rotation of the magnetizations of the two layers.

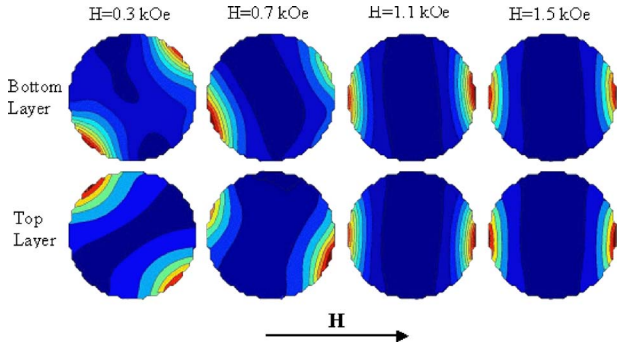

FIG. 5. (Color online) Magnetization profiles of the dynamic magnetization for the 0-EM mode in the two (top and bottom) NiFe disks for different values of the external field H applied along the arrow direction. The magnetic profiles are calculated using the procedure described in the text.

When the field is decreased down to zero, a good agreement is found between experiment and calculation with the exception of the modes which are localized near the edges of the magnetic elements, such as the 2-EM and the 0-EM mode. This is not surprising, since the frequencies of these modes are influenced to a large extent by the real morphology and curvature of the dot edges. This is reflected by the pronounced broadening of the experimental BLS peak of this mode (observed in the spectra of Fig. 3). In addition, in micromagnetic calculations, the dot edge is discretized, so that we expect the agreement between measured and calculated frequencies to be the worst where the discretized edge fails to mimic satisfactorily the actual rounded shape of the dot.

To gain further insights into the field evolution of the modes character, we present in Fig. 5 the profiles of the dynamic magnetization in the top and bottom NiFe disks for the 0-EM at different values of H. The character of this mode is particularly easy to identify, because it remains unchanged over the whole field range investigated. It is very interesting to observe how the localization region of the mode strictly follows the magnetization configuration of the layers and reflects their in-plane rotation. A similar in-plane rotation of the mode profiles occurs also for other modes. However, as soon as the magnetization in the two layers deviates from parallel alignment, it is not possible to follow a well-defined profile vs H, because the character of each mode becomes less and less defined, mode-crossings occur and different degrees of hybridization occur.

V. CONCLUSIONS

The static and dynamical properties of trilayered NiFe(10 nm)/Cu(10 nm)/NiFe(10 nm) disks have been studied. The hysteresis loop measured by Kerr magnetometry has been successfully reproduced by 3D micromagnetic simulations, revealing an antiparallel alignment of the layers magnetization at remanence, due to dipolar coupling between the NiFe layers. Concerning the dynamical properties, BLS measurements revealed the presence of several spectral features over a wide range of applied magnetic field. The

data interpretation required the calculation of the normal modes frequencies and profiles and an evaluation of the BLS cross section performing micromagnetic simulations. The experimentally revealed modes, were thus identified and classified depending on the phase-matching between the two layers and the distribution of the dynamic magnetization within each disk. The frequency dependence of the modes with the intensity of the applied magnetic field has been satisfactorily reproduced, giving evidence to the effect of the magnetization reorientation at sufficiently low field values. Also the evolution of the mode character with the field has been analyzed, showing that it is well preserved for field values above 0.5–0.6 kOe, while at lower field values hybridization effects make it difficult to follow the dynamic magnetization of a well-defined mode.

ACKNOWLEDGMENTS

The authors gratefully acknowledge financial support from the Italian Ministry for the Instruction, University and Research (MIUR), under FIRB and PRIN projects. The authors also acknowledge M. J. Donahue for the valuable support in the use of the OOMMF code.

*Present address: Dipartimento di Fisica, Università degli Studi di Perugia, Via A. Pascoli, 06123 Perugia, Italy. Electronic address: gubbiotti@fisica.unipg.it

[1] F. J. Himpsel, J. E. Ortega, G. J. Mankey, and R. F. Willis, Adv. Phys. **47**, 511 (1998); *Magnetic Nanostructures*, edited by H. S. Nalwa (American Scientific, Los Angeles, 2002); *Ultrathin Magnetic Structures III and IV*, edited by B. Heinrich and J. A. C. Bland (Spinger-Verlag, Berlin, 2005).

[2] S. E. Russek, S. Kaka, and M. J. Donahue, J. Appl. Phys. **87**, 7070 (2000).

[3] M. Grimsditch, L. Giovannini, F. Montoncello, F. Nizzoli, G. L. Leaf, and H. G. Kaper, Phys. Rev. B **70**, 054409 (2004).

[4] R. D. McMichael and M. D. Stiles, J. Appl. Phys. **97**, 10J901 (2005).

[5] L. Giovannini, F. Montoncello, F. Nizzoli, G. Gubbiotti, G. Carlotti, T. Okuno, T. Shinjo, and M. Grimsditch, Phys. Rev. B **70**, 172404 (2004).

[6] V. Novosad, M. Grimsditch, K. Yu Guslienko, P. Vavassori, Y. Otani, and S. D. Bader, Phys. Rev. B **66**, 052407 (2002).

[7] J. P. Park, P. Eames, D. M. Engebretson, J. Berezovsky, and P. A. Crowell, Phys. Rev. B **67**, 020403 (2003).

[8] F. Boust and N. Vukadinovic, Phys. Rev. B **70**, 172408 (2004).

[9] R. Zivieri and F. Nizzoli, Phys. Rev. B **71**, 014411 (2005).

[10] M. Buess, T. P. J. Knowles, R. Höllinger, T. Haug, U. Krey, D. Weiss, D. Pescia, M. R. Scheinfein, and C. H. Back, Phys. Rev. B **71**, 104415 (2005).

[11] K. Yu. Guslienko, W. Scholz, R. W. Chantrell, and V. Novosad, Phys. Rev. B **71**, 144407 (2005).

[12] B. A. Ivanov and C. E. Zaspel, Appl. Phys. Lett. **81**, 1261 (2002).

[13] S. O. Demokritov, B. Hillebrands, and A. N. Slavin, Phys. Rep. **348**, 441 (2001).

[14] J. Jorzick, S. O. Demokritov, B. Hillebrands, M. Bailleul, C. Fermon, K. Y. Guslienko, A. N. Slavin, D. V. Berkov, and N. L. Gorn, Phys. Rev. Lett. **88**, 047204 (2002).

[15] G. Gubbiotti, M. Kostylev, N. Sergeeva, M. Conti, G. Carlotti, T. Ono, A. N. Slavin, A. Stashkevich, Phys. Rev. B **70**, 224422 (2004).

[16] N. A. Sergeeva, S. M. Chérif, A. A. Stashkevich, M. P. Kostylev, and J. Ben Youssef, J. Magn. Magn. Mater. **288**, 250 (2005).

[17] K. Yu. Guslienko, K. S. Buchanan, S. D. Bader, and V. Novosad, Appl. Phys. Lett. **86**, 223112 (2005).

[18] M. J. Donahue and D. G. Porter, OOMMF User's Guide, Version 1.0, NISTIR 6376, National Institute of Standards and Technology, Gaithersburg, MD (Sept. 1999); http://math.nist.gov/oommf

[19] G. Gubbiotti, G. Carlotti, T. Okuno, T. Shinjo, F. Nizzoli, and R. Zivieri, Phys. Rev. B **68**, 184409 (2003).

[20] G. Carlotti and G. Gubbiotti, J. Phys.: Condens. Matter **14**, 8199 (2002).

[21] J. R. Sandercock, in *Light Scattering in Solids III*, edited by M. Cardona and G. Güntherodt (Springer-Verlag, Berlin, 1982), p. 173.

[22] G. Gubbiotti, M. Madami, S. Tacchi, G. Carlotti, and T. Okuno, J. Appl. Phys. **99**, 08C701 (2006).

[23] A spin wave is associated with the oscillation of two transversal components of the magnetization. In our case, since the magnetizations of the two layers are not always collinear with H and rotate in the *XY* plane, the dynamic magnetization components have three components in the Cartesian coordinate system we used (inset of Fig. 1).

[24] C. Kittel, Phys. Rev. **73**, 155 (1948).

[25] G. Gubbiotti, G. Carlotti, T. Okuno, M. Grimsditch, L. Giovannini, F. Montoncello, and F. Nizzoli, Phys. Rev. B **72**, 184419 (2005).

[26] K. S. Buchanan, K. Yu. Guslienko, A. Doran, A. Scholl, S. D. Bader, and V. Novosad, Phys. Rev. B **72**, 134415 (2005).